Thermal behaviour evolution of an IGBT module after aging measured by thermoreflectance

Youssef Metayrek, Thierry Kociniewski, Zoubir Khatir

Version of Record: https://www.sciencedirect.com/science/article/pii/S0026271420305837
Manuscript_acd66109870fa5d3780b48d8d03fe0db

Thermal Behaviour Evolution of an IGBT Module after Aging Measured by Thermoreflectance

Y.Metayrek[a], T.Kociniewski[b], Z.Khatir[a]

[a] *SATIE lab., IFSTTAR, 25 Allée des Marronniers 78000, Versailles, France*
[b] *Groupe d'Etude de la Matière Condensée (CNRS and University of paris SACLAY), 45 avenue des Etats-Unis, 78035, Versailles cedex, France*

Abstract – In this paper, we propose to study the thermal mapping evolution of the Insulated gate bipolar transistor (IGBT) emitter metallization after aging by thermoreflectance. Thermoreflectance measurements were done in static regime before and after aging by DC power cycling. The aim of this study is to observe the change in thermal behaviour at the cell level due to power cycling aging. Preliminary results indicate that a pixel-by-pixel calibration which takes into account the topography and chemical changes of the metallization is essential to eliminate artefacts in thermal images and to allow to follow metallization thermal evolution with aging.

1. Introduction

IGBT modules have become key devices in several applications. Currently they are widely used in industrial technology, aerospace electronic devices and transportation [1-2]. Considering the growing place of IGBT power modules in these applications [3-4], the reliability of systems is paramount. This reliability is affected by a variety of application-specific factors such as electrical load and environmental conditions (temperature, humidity).

In any experimental study concerning the reliability of power IGBT modules, the first objective is to reproduce the thermal and electrical stresses that these components could undergo in a real application such as transport applications. Accelerated aging tests, such as power cycling, are often used to reproduce the thermal stresses induced by the self-heating of the power module. These tests should lead to the understanding of the physical mechanisms of degradation and aging of electronic power IGBT modules, and to improve the reliability of the component. Usually these tests lead to degradation of the chip metallization and the wire bondings on the top surface of IGBTs. Therefore, it is important to study how the degradations will affect the thermal behaviour in the chip environment.

Generally, the thermal behaviour in the chip is summarized by a thermosensitive electrical parameter (TSEP) like the junction temperature (T_j) [5]. Nevertheless, the junction temperature is a virtual value corresponding to a "mean" value inside the chip. Thus, this electrical parameter is well-suited for monitoring a global thermal indicator but not for temperature distribution measurements considering the temperature gradients that can take place in the chip active areas. It is necessary to orient the choice towards other mapping techniques like optical methods.

Optical methods are the best solution to obtain the temperature distribution on the IGBT surfaces with high spatial and temperature resolution. Among the available optical methods one can use infrared imaging (IR) [6], micro-Raman spectroscopy [7] and thermoreflectance [8]. Infrared imaging is a well-known method which requires removing the silicone gel used as an encapsulant in power modules, in order to have direct access to the surface of the chip. This has the consequence of preventing the thermal characterization in high voltage operations, and thus in real operating conditions. Additionally, it is necessary to coat the sample with a thin film of black paint to homogenize the surface emissivity. As drawback of this coating that is can modify the thermal response in high transient operations [9]. In another way, Raman spectroscopy cannot be used to characterize metals and requires a point-to-point measurement of the analysed area which can last several minutes for each point. Thermoreflectance does not have these previously mentioned faults. It is a non-contact and non-destructive technique, that can be used for both steady-state and transient surface temperature measurements and can provide accurate results with spatial resolution up to 250 nm and a thermal resolution of 10 mK [8]. This technique adapts perfectly to the thermal measurement of metallized surfaces chips in power modules.

Thermoreflectance microscopy is based on the measurement of the relative change in the device surface reflectivity (R) as a function of temperature. When the temperature of the sample changes, the refractive index changes, as well as the reflectivity. For most materials (semiconductors and metals), this relationship can be approximated to the first order by:

$$\frac{\Delta R}{R} = \frac{1}{R}\frac{\partial R}{\partial T}\Delta T = k\Delta T \quad (1)$$

With (ΔR) is the variation of the reflectivity at the surface of the component. The coefficient k is called the thermoreflectance coefficient and it generally varies between 10^{-2} and 10^{-5} K^{-1}. The thermoreflectance coefficient depends on several factors like the illumination wavelength, the nature of the materials, the topography and the numerical aperture of the objective [10]. Thus, a precise and local measurement of this coefficient is essential to obtain a good estimation of absolute temperatures at the surface of the component.

In this paper, we use thermoreflectance to study the evolution

of temperature distribution on IGBT emitter metallization with aging. A pixel by pixel calibration was used in order to correct the thermoreflectance calibration coefficient evolution due to metallization aging. Thus, emitter metallization temperature distribution of a cycled and uncycled module could be compared and the effect of the aging of the metallization on the thermal distribution can be highlighted.

2. DC Power cycling

In practice, a power cycling test is produced by injecting a power current for a duration (T_{on}) followed by stopping the injection of this current for a duration (T_{off}) in order to induce heating phases and controlled cooling in the module. Thus, a temperature variation ΔT_j corresponding to a cycle of a duration $\{T_{on} + T_{off}\}$ is obtained. This temperature cycle is repeated until the appearance of degradations or reaching an end-of-life criterion as the number of failure cycles noted N_f. There are several strategies for power cycling test that lead to different life time estimates. The main strategies are those with constant current, constant power P, and constant temperature variations ΔT_j [11].

In our case, power IGBT module have been tested in power cycling conditions at high ambient temperature. The accelerated power cycling tests in DC-mode have been done on a module with test conditions in junction temperature swing ΔT_j= 110K and $T_{j\,min}$=55°C. The total current injected was 260 A. The duration of the power injection and cooling phases (Ton) and (Toff) were fixed respectively at 3 s for the heating time and 6 s for the cooling time. Figs. 1(a) and 1(b) present optical images of IGBT emitter metallization taken by a microscope at x10 magnification before and after 100000 cycles. Direct comparison between the two images show how the chip metallization have evolved. Fig. 1(b) shows the IGBT emitter metallization degradation which topography have completely change and roughness increased. This degradation is well known and is due to visco-plastic behaviour of aluminium grains during temperature cycling [12].

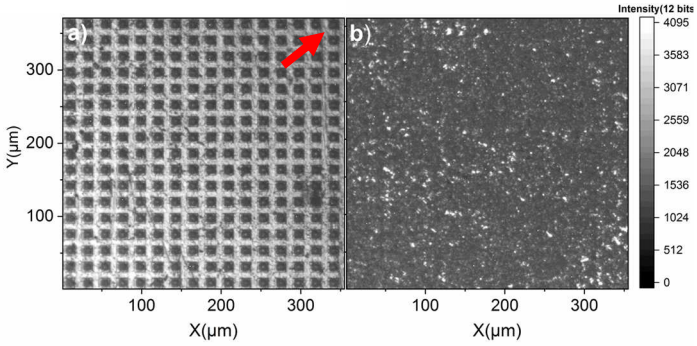

Fig. 1. Optical images at x 10 magnification a) Uncycled IGBT chip emitter metallization. The red arrow indicates the bonding position b) IGBT chip emitter metallization after 100000 power cycles.

3. Thermoreflectance measurements

3.1 Methodology

Thermoreflectance measurements were carried out on uncycled and cycled IGBT emitter metallisation in homodyne conditions. Fig. 2 presents the basic setup of a homodyne Charge Coupled Device (CCD) based thermoreflectance. In this setup, the IGBT module is excited by a sinusoidal electrical signal V_{ce} at a given frequency F which creates a warm-up at the same frequency while a continuous illumination is applied by a light emitting diode (LED) source focused on the sample by a microscope objective. Light is reflected to a CCD camera and images are collected by a computer at a frequency 4F. Taking 4 images per excitation cycle and averaging them provides access to the variation of the reflectivity of each pixel by making a simple calculation on the mean intensities as described in [13].

$$\frac{\Delta R}{R_0} = \frac{\pi}{\sqrt{2}} \frac{\sqrt{(\Sigma I_1 - \Sigma I_3)^2 + (\Sigma I_2 - \Sigma I_4)^2}}{\Sigma I_1 + \Sigma I_2 + \Sigma I_3 + \Sigma I_4} \qquad (2)$$

Where ΣI_1, ΣI_2, ΣI_3 and ΣI_4 are the sum of each images 1, 2, 3 and 4 taken in each heating period.

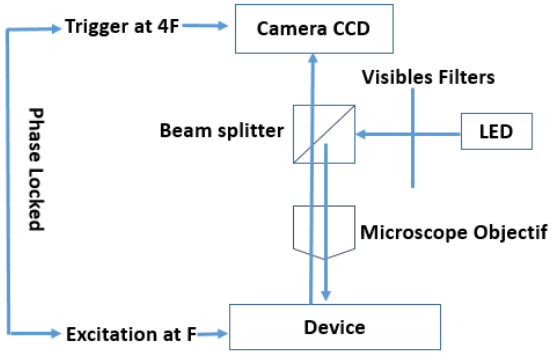

Fig. 2. Schematic description of a homodyne thermoreflectance microscopy setup.

3.2 Measurements

The frequency of electrical excitation determines the shape of the thermal signal. In order to apply the Eq. (2), it is necessary to obtain a sinusoidal thermal signal from electrical excitation. For frequencies lower than or equal to 0.625 Hz, the thermal excitation matches perfectly the form of sinus function [14]. Thermoreflectance images were made in static regime at F=0,625 Hz. Electrical conditions were adjusted to inject the same power 20 W in uncycled and cycled module. This limited power was chosen in order to keep the device in focal plan of the objective. It should be noted that this problem will be solved in the future by using a proportional derivative controller integrated into the target z [15]. The second advantage of this low power is to avoid carrying out an additional unintentional cycling of the module.

Figs. 3 present thermoreflectance images of a 360 µm x 360 µm IGBT emitter metallization before and after cycling at the same dissipated powers 20 Watts. The thermoreflectance

measurements were performed at x10 magnification with a wavelength of 632 nm. Since averaging series of four images increases the dynamics of the measurements [16], we have averaged the signals over 500 periods. These measurements were made in the edge of the chip near the wire bond contact. The red arrow in the optical image of the uncycled module (fig. 1.a) at the top right indicates the bonding position.

In Fig. 3a), hot areas appear in the centre of the structures (elementary cells) which could be identified to the active part of the components. Details of the structure of these cells are presented in [17]. Considering that the whole surface is aluminum, a unique and constant calibration coefficient could be used which will lead to consider the reflectivity image as a thermal image. But this extrapolation could introduce interpretation errors because the surface is not planar and the use of different calibration coefficients is necessary depending on the topography of the surface.

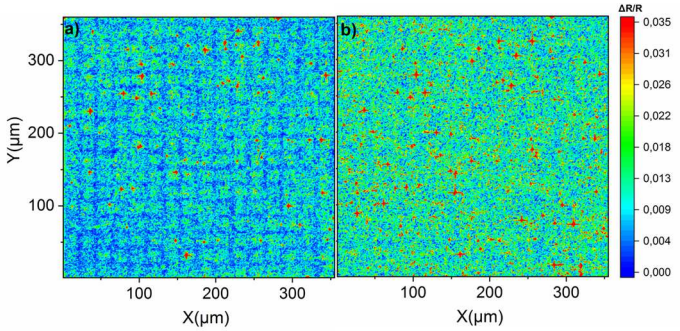

Fig. 3. Thermoreflectance images ΔR/R obtained on IGBT emitter metallization: a) before aging b) after aging.

In Fig. 3b) fewer gradients appear in reflectivity image due to the restructuring of the metallization with aging which creates a more homogeneous topography: rougher but without significant drops. (ΔR/R) image in cycled case presents higher intensities than in uncycled case which might suggest that the metallization after aging is warmer. The metallization has also changed between the uncycled and cycled module and a different calibration is necessary. Thus, it is not possible also to compare directly the thermoreflectance images (ΔR/R) before and after aging without performing pixel by pixel calibration in each case.

4. Pixel by pixel calibration and thermal measurement

In order to study the evolution of the IGBT emitter metallization temperature with aging, it is important to make a pixel by pixel calibration. In this calibration method, thermoreflectance coefficients were extracted independently for each pixels. Note that the calibration and the thermoreflectance measurement must be done exactly in the same area of interest so that each thermoreflectance coefficient corresponds to the correct pixel of the reflectivity image.

In our case, the calibration methodology was done in several steps. First, the IGBT module was mounted on a temperature controller consisting in a Peltier system Linkam PE120. This system can control temperatures from -25 ° C to 120 °C with an accuracy of +/- 0.1 ° C. The temperature was fixed to a value and we waited until the thermal equilibrium of the IGBT module was reached (around 10 minutes). In order to confirm that the temperature was reached and is homogeneous on the surface of the component, thermal measurements were made at different place of the chip using a thermal sensor made up of a GaAs crystal, described in [10]. After temperature stability was obtained, we set up the focus and corrected the lateral movements due to the surface displacement with thermal dilatation. Finally, the average intensity of each pixel was measured by taking several thousand images in order to reduce the photon noise.

By repeating this procedure for different fixed temperatures, it was possible to plot intensity (I/Iref) as a function of temperature (T) for each pixel. A linear fit permitted to extract the thermoreflectance coefficient of each the pixel. A program was developed on Matlab to automate calculations.

A fit example of an arbitrary pixel is presented in fig. 4 using 4 temperatures. This curve shows a good linearity between (I) and (T), and the slope give the thermoreflectance coefficient. The fits have a coefficient of determination (COD) varying between 0.85 to 0.98 for the uncycled metallization and 0.92 to 0.98 for the cycled metallization. This difference is explained by the strong topographic variations of the uncycled metallization at the level of elementary cells which disturb the reflected signal.

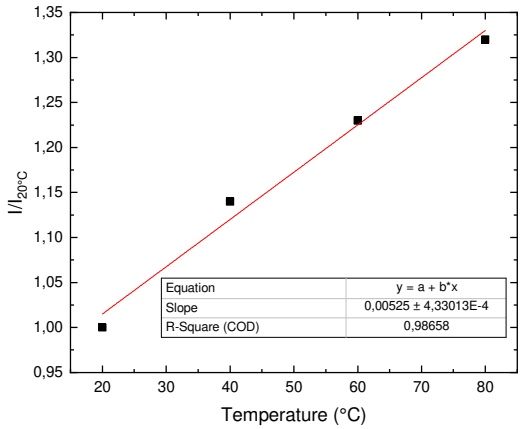

Fig. 4. Linear fit obtained for one pixel with 4 normalized intensities measurements corresponding to 4 different temperatures.

Repeating the fitting for each pixel, we obtained the matrix of the thermoreflectance coefficient which has the same dimension of the optical image.

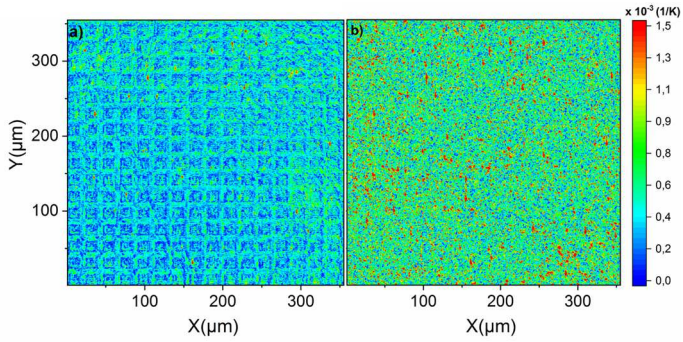

Fig. 5. Pixel by pixel calibration map coefficients obtained at 632 nm wavelength on the IGBT emitter metallization a) before aging and b) after aging.

Fig. 5a presents the map of thermoreflectance coefficient k obtained on an uncycled IGBT emitter metallization. Calibration coefficients have close values in the plane intercellular regions and these values change radically (divided by 4) in the area of the cells where the topography varies a lot. Same image is presented in fig 5b) for the cycled metallization. The thermoreflectance coefficients are more homogeneous and the values are closer to those obtained on the flat areas of the uncycled metallization. Note that the mapping of thermoreflectance coefficients reflects the topography variations observed in the optical image of the surfaces. This clearly shows the dependence of the calibration coefficient on the nature of the surface.

From the image (ΔR/R) and the corresponding matrix of thermoreflectance coefficients k, it was possible to obtain the calibrated thermal mapping (ΔT) of the surface by dividing each pixel value of the mapping (ΔR/R) by the value of k corresponding.

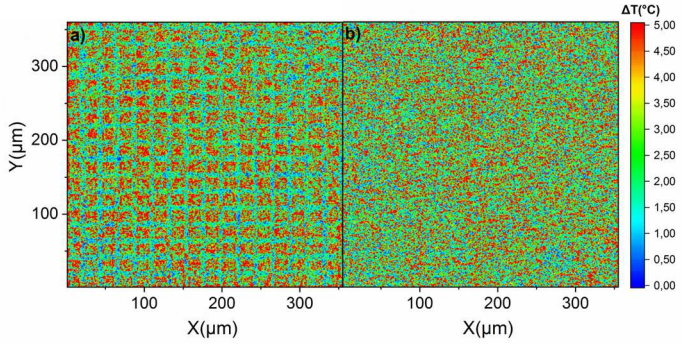

Fig. 6. Calibrated thermal image obtained on IGBT emitter metallization a) before aging and b) after aging.

Figs. 6 present the calibrated thermal images obtained on the IGBT metallization before and after aging for 20 W dissipated power. Real hot zones are now revealed. The hot spots no longer correspond between (ΔR / R) and the thermal images. For the uncycled module, it can be seen that the active zones in the center of the cells appear clearly warmer than in the intercellular zones. These thermal gradients decrease as we approach a bonding. For the cycled module, the thermal distribution is more homogeneous. The active areas are less thermally marked. This could be explained by the local metallization restructuration. Indeed, the structure of the metallization observed in the optical images shows that the metallization would have thickened at the level of the cells by the disappearance of the steep zones. The local heating would thus be homogenized in the thickness of the metallization. It is important to specify that the couple (V_{ce} , I_{ce}) corresponding to the 20 Watts injected have remained identical between the cycled and uncycled module, which suggests that only the emitter metallization structure has been affected by this aging. We have also calculated the average temperatures of the two surfaces and they were substantially equal to 4.1 °C.

Thermoreflectance is an interesting technique for power components thermal studies. It offers high resolution measurements without any preparation. However, a pixel-by-pixel calibration is necessary in the case of inhomogeneous surface or complex structure to obtain local calibrated temperature in order to be able to compare regions with different compositions or topographies like in aging studies. Thanks to its spatial and thermal resolution due to the averaging of the measurements, the thermoreflectance should be able to provide thermal measurements making it possible to support the analytical models of aging.

5. Conclusion

In this paper the effect of power cycling aging on the temperature map at the top surface of IGBT in module was presented. Measurements were done at the cell scale. The comparison of thermal maps between uncycled and cycled module were only possible due to the use of a pixel-by-pixel calibration. First results show that thermoreflectance images ΔR/R introduce error in hot spots localization but the pixel-by-pixel calibration reveals real heating zones considering the inhomogeneity of thermoreflectance coefficients values. Thus, the heating zones at the level of the cellular structure of IGBT chips have been highlighted. The comparison of the two thermal maps has showed that the average temperatures of the two surfaces at constant injected power are substantially equal and the temperatures are much more homogeneous in the case of aged metallization.

References

[1] X.Perpina et al., “IGBT module failure analysis in railway applications” Microelec. Reliab., vol. 48, no. 8-9, pp. 1427-1431, 2008.

[2] A. Nakagawa, Y. Kawaguchi and K. Nakamura.,“Silicon limit electrical characteristics of power devices and Ics”, ISPS, 2008.

[3] H. Lu, C. Bailey and C. Yin, “Design for reliability of power electronics module”, Microelec. Reliab.,vol. 49, pp. 1250-1255, 2009.

[4] S.Vanessa et al., “Ageing and Failure Modes of IGBT Modules in High-Temperature Power Cycling”, IEEE Trans. Ind. Electron., vol. 58, no. 10 , pp. 4931-4941, 2011.

[5] M. Halick, M. Sathik, J. Pou, S. Prasanth, V. Muthu, R.Simanjorang and A.K. Gupta , “Comparison of IGBT junction temperature measurement and estimation methods-a review”, 2017 Asian Conference on Energy, Power and Transportation Electrification (ACEPT) , 2017.

[6] A. Irace,“Infrared Thermography application to functional and failure

analysis of electron devices and circuits" , Microelectron. Reliab., vol.52 , no. 9-10, pp. 2019-2023, 2012.
[7] T. Kociniewski, J. Moussodji and Z. Khatir, "Temperature mapping by l-Raman spectroscopy over cross-section area of power diode in forward biased conditions", Microelectron. Reliab., vol. 55 , pp.547–551, 2014.
[8] M. Farzaneh, et al.,"CCD-based thermoretlectance microscopy: principles and applications" ,Phys. D: Appl. Phys. , vol. 42, pp.143001 (20pages), 2009.
[9] G. Ptaszek et al., "Transient thermography testing of unpainted thermal barrier coating (TBC) systems, NDT & E International", NDT & E International, vol.59 , pp. 48-56, 2013.
[10]G.Tessier et al.,"Quantitative thermal imaging by synchronous thermoreflectance with optimized illumination wavelengths", Appl. Phys. Lett., vol.78 , pp.2267-2269, 2001.
[11] Kovacevic.I.F et al., "Modelling for the lifetime prediction of power semiconductor modules" Reliability of Power Electronic Converter Systems, chap. 5, pp. 1-43, 2015.
[12] M. Bouarroudj et al.,"Degradation behavior of 600 V–200 A IGBT modules under power cycling and high temperature environment conditions", Microelec. Relia., vol. 47, pp. 1719–1724, 2007.
[13] P. M. Mayer et al., "Theoretical and experimental investigation of the thermal resolution and dynamic range of CCD-based thermoreflectance imaging ",J. Opt. Soc. Am. , vol.24, pp.1156-1163, 2007.
[14] Y. Metayrek et al ,"Thermal Mapping at the cell level of Chips in Power Modules through the Silicone Gel Using Thermoreflectance ", Microelec. Relia., vol. 105, pp. 113563, 2020.
[15] S. Dilhaire, S. Grauby and W. Claeys,"Calibration procedure for temperature measurements by thermoreflectance under high magnification conditions", Appl. Phys. Lett. , vol.84 , pp. 822-824, 2004.
[16] G. Tessier, M. Bardoux, C. Filloy, C. Boué and D. Fournier, " High resolution thermal imaging inside integrated circuits", Sensor Review, vol. 27, no.9-10, pp.291-297, 2007.
[17] S.Azzopardi and A.Benmansour " Low temperature Trench IGBT static and dynamic operating modes investigation based on simulation and
experiments", 2011.